Available online at www.sciencedirect.com

ScienceDirect

Advances in Space Research 67 (2021) 4043–4053

ADVANCES IN SPACE RESEARCH (a COSPAR publication)

www.elsevier.com/locate/asr

Second order experimental statistics of rain attenuation at Ka band in a tropical location

Swastika Chakraborty [a], Madhura Chakraborty [b], Saurabh Das [c,*]

[a] Sikkim Manipal Institute of Technology, Sikkim Manipal University, Rangpo 737136, India
[b] JIS College of Engineering, Kalyani, Nadia 741235, India
[c] Discipline of Astronomy, Astrophysics and Space Engineering, Indian Institute of Technology, Khandwa Road, Simrol, Indore 453552, India

Received 30 September 2020; received in revised form 10 February 2021; accepted 24 February 2021
Available online 12 March 2021

Abstract

Some second order rain attenuation statistics such as fade duration and fade slope are investigated on the basis of experimental measurements of received signals using the GSAT-14 satellite beacon signal at 20.2 GHz for three years (2014–2016) over the tropical location Ahmedabad (23.02 ^{0}E, 72.51^{0}N), India with an Elevation angle of 63^0. Existing models of fade duration are compared with experimental data in this study and exponent of power law model of fade duration at Ka band is further explored. A new model for fade duration for Ka band for tropical locations is proposed where the constant of exponent of attenuation in the power law is found to be 0.143 instead of 0.055 used in ITU-R. Other relevant parameters for implementation of fade mitigation technique to prevent the link outage like cumulative distribution of signal fade rate, maximum and minimum fade rise and fade fall are also studied. Fade slope asymmetry over tropical region is also investigated. Keeping in view of exploiting the commercial launch of Ka band in Indian region there is an urgent need for validation of the existing models of fade slope (specially looking into fade symmetry) and fade duration. It will help the SATCOM (Satellite Communication) link designer to improve closed loop fade mitigation technique to minimize the possible link failure/link outage over the tropical region.

Keywords: Fade Duration; Ka band Beacon Measurements; Satellite Communication; Tropical region; Fade slope asymmetry

1. Introduction

Availability of a high capacity radio communication link maintaining good quality of service (QOS) demands optimum fade mitigation technique (FMT) to be adopted with adequate tracking speed while designing Earth- space communication link above 10 GHz. In order to optimize the system resource sharing, the second order statistics of rain attenuation i.e. rain induced fade durations and fade slopes, are important parameters and needed to be modeled as accurately as possible. This will also help in better tracking speed of FMT and proper estimation of link outage time. Fade duration is the time duration for which attenuation remains higher than a threshold value. Fade slope, on the other hand, is quantified as the change of attenuation per unit time. Both fade duration and fade slope primarily depend on attenuation value, however slope is also strongly dependent on sampling time and climatic condition while duration depends on frequency and elevation angle of the link in addition to the attenuation threshold.

Optimum SATCOM link design and selection of appropriate FMT above 10 GHz requires exhaustive knowledge of these above mentioned two parameters. Especially For-

* Corresponding author.
E-mail addresses: saurabh.das@iiti.ac.in, das.saurabh01@gmail.com (S. Das).

https://doi.org/10.1016/j.asr.2021.02.033
0273-1177/

ward Error Correction (FEC) coding scheme and proper modulation scheme selection requires very accurate information on dynamic nature of rain attenuation. Even short duration and long duration of rain events (attenuation and scintillation both) are of separate importance while designing FMT to counter rain attenuation as well as scintillation. Similarly, application of Uplink Power Control (ULPC) as a FMT needs the quantification of dynamic range of attenuation. However, a very few measurements using the satellite links at Ka and above frequencies (such as INTELSAT VI) are reported over the tropical climate (Allnutt and Rogers, 1990). Experimental studies were also carried out in the Ka and Q/V bands for the verification of existing fade countermeasure techniques based on the measurements from ESA OLYMPUS and ASI ITALSAT satellites (Paraboni et al., 2007). In another study, statistical performance analysis of both fade slope and duration have been presented (Zemba et al., 2018) using simultaneous measurement at 40 GHz and 20 GHz at Edinburgh, Scotland.

Fade duration prediction model proposed by Paraboni and Riva (Paraboni and Riva, 1994) has been already included in the ITU-R model. Several other fade duration prediction models at Ku band (Lekkla et al., 1998; Matricciani, 1981; Matricciani, 1996; Timothy et al., 2000) and at Ka band (Timothy et al., 1998; Bråten et al., 2001) for the frequency range of 20 GHz to 40 GHz are also reported. Fade duration prediction in Q-band using Alphasat (Pimienta del Valle et al., 2018) are also reported over temperate climate. However, since most of the models based on signal strength data at Ka band are from temperate regions, there are still not enough information of the performances of the existing models over tropical regions. Especially, performance evaluation of the models that can predict the fade duration distribution from rain rate distribution (Paulson and Gibbins, 2000; Kormanyos et al., 2000) may be useful in absence of beacon measurement. This is particularly true for tropical regions which are very less studied.

In another literature (Mandeep, 2013) the prediction of the models (ITU-R P.1623 –1, 2005, Kormanyos et al., 2000, Paulson and Gibbins, 2000) have been compared with the measured data of fade duration over the equatorial region. Another work (Dao et al., 2018) also compared the performance of the popular fade duration models (ITU-R P.1623 –1, 2005, Timothy et al., 1998, Cheffena and Amaya, 2008) at Ku band over tropical climate and proposed a new model. However, the modification is done on the basis of unfiltered data i.e. the input data of rain event mixed with the data of scintillation event.

On the other hand, exhaustive studies of fade slope at Ku band (Matricciani, 1981; Nelson and Stutzman, 1996; Timothy et al., 2000) and at Ka band (Sweeney and Bostian, 1992; Van de Kamp, 2003; Nelson and Stutzman, 1996) are reported in literature in addition to ITU-R (ITU-R P.1623 –1, 2005) model using the measurements mostly over the temperate climate from several satellites such as of ETS (Timothy et al., 2000), SIRIO (Paraboni and Riva, 1994), COMSTAR (Timothy et al., 2000), Olympus (Paraboni et al., 2007; Nelson and Stutzman, 1996), ACTS (Crane and Robinson, 1997), Italsat (Paraboni et al., 2007) etc. Using the beacon signal from satellite OLYMPUS (Van de Kamp, 2003) and satellite MEASAT 3 (Dao et al. 2012) fade slope prediction models are also developed. Some analyses are also available in literature for fade slope analysis of Ka band (Das et al., 2020) to V band using the data from temperate region (Chambers et al., 2006; Vilhar et al., 2016).

However, there is a very few fade slope prediction study (Chakraborty et al., 2020) available at Ka band and above for the validation of the dynamic parameters over tropical region. Some literature (Sujimol et al., 2015) validated existing ITU-R model using the beacon of IPSTAR in Ka band and GSAT-8 in Ku band. Some studies have been carried out on the fade slope asymmetry due to convective precipitation using beacon signal of Measat-3 over equatorial Malaysian site (Jong et al., 2014, Jong et al., 2019) at Ku band.

Keeping in view of exploiting the commercial launch of Ka band in Indian region there is an urgent need for validation of the existing models of fade slope and fade duration. It will help the SATCOM (Satellite Communication) link designer to improve closed loop fade mitigation technique to minimize the possible link failure/ link outage over the tropical region.

2. Data source

The 20.2 GHz beacon signal data from GSAT-14 has been obtained from Space Applications Center, Indian Space Research Organization, collected over Ahmedabad (23.02 °E, 72.51°N) Earth Station by an antenna of 2.3 m diameter having 21.7° polarization angle and 63° elevation angle for three years (2014–2016). The antenna height above mean sea level is 49.7 m and station height is 48.7 m. Collocated rainfall data were collected using a disdrometer and a tipping bucket rain gauge with 1 min integration time. The average rain fall intensity for this location is observed to be 42 mm/hr for 0.01% time in a year with 1 min integration time.

2.1. Data preprocessing

The received signal data obtained at 20.2 GHz with a sampling rate of 1 Hz is collected and used for further analysis. Fade slope analysis is carried with filtered data and fade duration analysis is carried out with unfiltered data having both attenuation and scintillation. For fade slope calculations, first the abrupt fluctuations of signal due to temperature variation and/or due to mechanical and human error are removed by visual inspection. After that the data is filtered to remove the fast fluctuation (i.e. scintillations) by using a 10th order Butterworth low pass filter of appropriate cut-off frequency. The cut-off frequency is

estimated as 0.025 Hz by the spectral analysis of actual data as shown in Fig. 1. Both unfiltered and filtered data are later used, one for fade duration and other for fade slope analysis, consecutively.

During the calculation of attenuation, rainy and non-rainy days are separated first. Non-rainy days are identified from visual inspection of signal level. This process is repeated for three years on 20.2 GHz data .This signal level values of non-rainy days in each month are later on averaged. This averaged non-rainy clear sky signal level is filtered with same cut off frequency that has been used for rainy day for removing the scintillation. This clear sky level is the reference signal level. Finally total attenuation is calculated by taking the difference between reference signal level (dB) and measured signal level (dB) during rain. Fig. 2 shows an example of such data processing steps for a typical rain attenuation event of almost one hour of 19th August 2016 over Ahmedabad along with the rain rate information.

As attenuation due to rain is the major contributor among those due to atmospheric components, it is mentioned here as rain attenuation (Das et al., 2020). The 20.2 GHz data is collected for consecutive three years from 2014 to 2016 with a data gap during August and October in 2015, and December 2015 to February 2016 causing 86% availability of data. It is to be noted here that in Ahmedabad, rain mostly occurs during monsoon period and, in fact, only 8 days of rain data (i.e. ~ 6% of total rainy days) are missing out of total 134 rainy days over 3 years period. As the present work is focused on the rain attenuation, the missing data will therefore have very less contribution in final statistics and may be accounted as year-to-year natural variability of rainfall. Hence, the average year's statistics is generated based on total measurement period.

3. Methodology and results

3.1. Dynamic analysis of rain attenuation

Two important dynamic characteristics namely fade slope and fade duration are studied here in details. Slope of rain-induced fade is primarily required as the tracking parameter for FMT to be adopted. Rain-induced fade slope is quantified as (Van de Kamp, 2003)

$$\zeta(t) = \frac{A(t + 0.5\Delta(t)) - A(t - 0.5\Delta(t))}{\Delta(t)} \quad (1)$$

where A is the attenuation and $\Delta(t)$ is the time interval for which the fade slope has been calculated. For this work, data of 1 sec temporal resolution have been used for estimating the fade slope and the time interval (Δt) considered over here is 2 sec.

The duration of rain attenuation event is defined as the time duration of exceeding a particular attenuation threshold by the received signal continuously. Probability of occurrence of fade duration d longer than a given duration D, above given attenuation threshold A (ITU-R P.1623 –1, 2005) is

$$P(d > DIa > A) = \frac{N(d > DIa > A)}{N_{tot}(A)} \quad (2)$$

where $N_{tot}(A)$ is the total number of fade events exceeding the attenuation threshold A, and $N(d > DIa > A)$ is the number of fade events distribution.

3.2. Symmetry of fade slope at Ka band

In ITU-R model, it is assumed that there is no significant change in the slope distribution in positive or negative

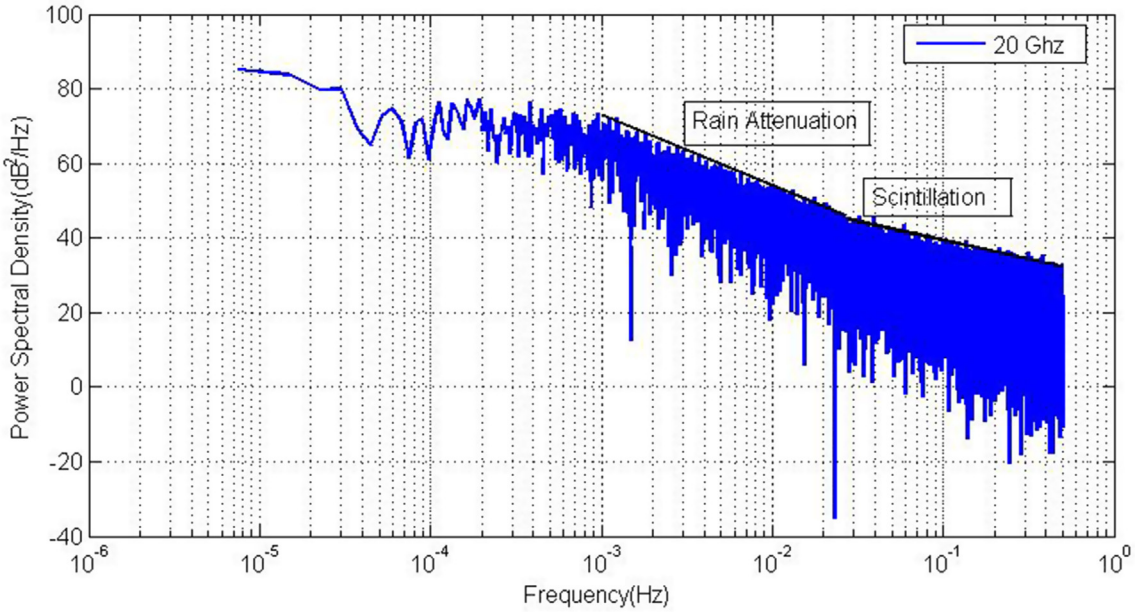

Fig. 1. Power Spectral Density of the rain attenuation and scintillation (20.2 GHz) for the year (2014–2016), Ahmedabad, India.

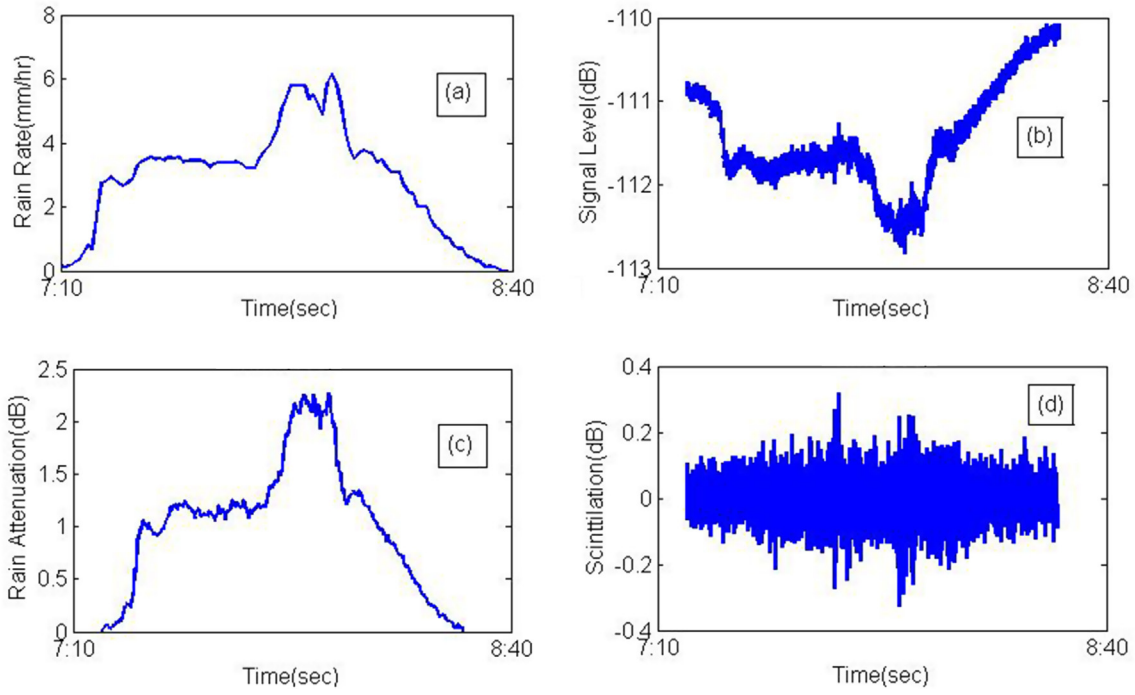

Fig. 2. Data processing steps for a typical attenuation event (19th August 2016) (20.2 GHz), Ahmedabad, India, (a) Rain rate (mm/hr), (b) Signal Level (dB), (c) Rain Attenuation (dB), (d) Scintillation (dB).

direction. Therefore, the fade slope model is symmetrical and depends only on the attenuation value and filter characteristics. Hence, it is worth investigating if the same assumptions are valid over tropical regions as well or not. The attenuation data available from the received signal of three years are used to calculate the fade slope by equation (1). The attenuation threshold of 3 dB, 6 dB, 9 dB, 12 dB and 15 dB are considered here. For each attenuation threshold, fade slope time series is then calculated. Cumulative distribution of fade slope from measured data and using ITU-R (ITU-R P.1623 –1, 2005) are shown for three-attenuation threshold level i.e. 3 dB, 9 dB and 15 dB in Fig. 3. It is observed that the ITU-R model (ITU-R P.1623 –1, 2005) is performing well in estimating fade slope over Ahmedabad. Here standard deviation of fade slope for a particular attenuation threshold is the only deciding parameter and for 3 dB and 9 dB the measured and calculated standard deviation of fade slope using ITU-R (ITU-R P.1623 –1, 2005) are matching very closely. However, at higher attenuation threshold like 15 dB, slight difference is observed. This may be due to change in nature of rain or may be due to limited observation of high rain attenuation.

For detailed analysis of the fade slope and its symmetry, the whole fade slope is then split into positive fade slope and negative fade slope. This analysis is more informative than analysis of standard deviation for system design. The positive fade slope and negative slope are mentioned as fade rise rate and fade fall rate over here. In Fig. 4, the variations of mean value of fade rise and fade fall rate are shown for different attenuation thresholds. It is seen that at least up to 10 dB attenuation threshold, both of fade rise and fade fall rate, show a monotonic increase with attenuation threshold. But after 10 dB, differences in mean value between fade rise rate and fade fall rate are evident. That is the clear indication of non-symmetrical nature of positive and negative fade slope distribution (Chambers et al., 2006). This also indicates that the non-symmetry is due to the nature of rain of tropical region. Though due to limited number of samples present at higher attenuation threshold, more analysis is necessary to reach to any conclusion. For better understanding of the slope asymmetry, cumulative distribution of fade rise rate and fade fall rate for any single attenuation threshold are plotted in Fig. 5. This shows very clearly that at the high value of fade slope and high value of attenuation threshold, the departure between CDF of fade rise rate and fade fall rate widens and may be because of convective type of rain (Chambers et al., 2006). Higher attenuation threshold shows greater asymmetry and in 15 dB attenuation threshold, the deviation between CDF of fade fall and fade rise rate is more than the differences observed in 3 dB.

3.3. Fade duration analysis at Ka band

Fade duration is another key information for selection of appropriate FMT and for the optimum sharing of system resources. Proper knowledge of fade duration will help in choosing proper coding scheme for error correction such as size of coding word and interleaving in concatenated code. As knowledge of fade duration is required to be

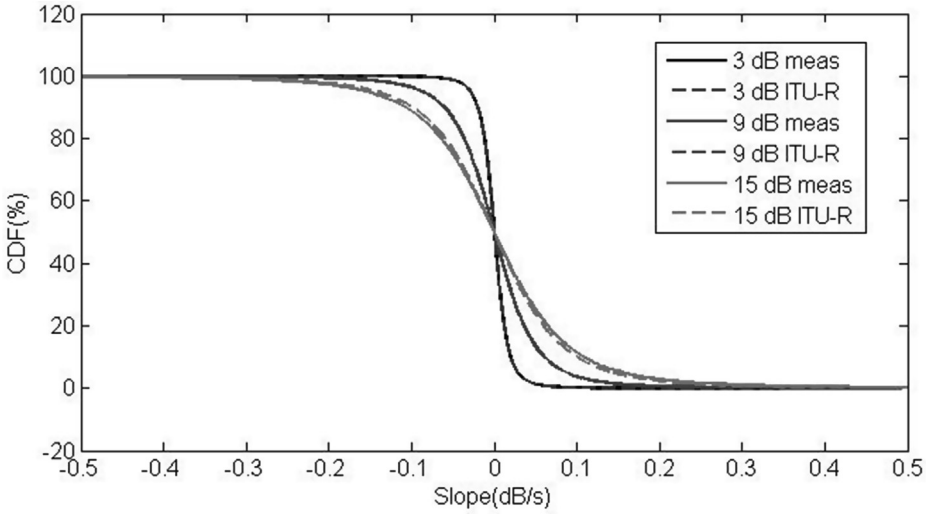

Fig. 3. Cumulative distribution of measured fade slope at 20.2 GHz (2014–2016) (plain line) compared with ITU-R model developed fade slope(dashed lines) for different Attenuation (dB) threshold (Ahmedabad).

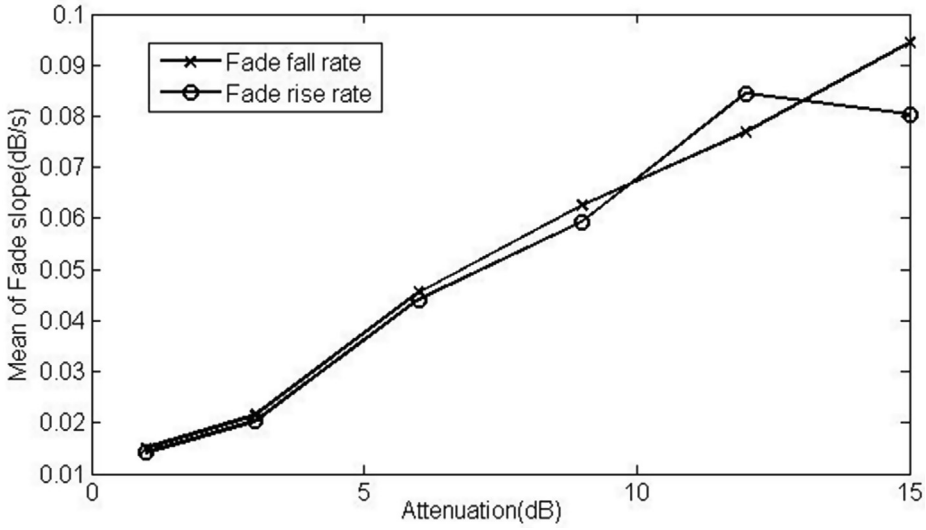

Fig. 4. Mean value of fade slope (both fade fall rate and fade rise rate) at 20.2 GHz (2014–2016) for different attenuation threshold (Ahmedabad).

known with a higher degree of precision, general practice is to subdivide the entire fade duration available for the experiment into long and short duration fades. Due to the sampling rate of 1 Hz, the fade duration longer than 1 sec is considered here for all calculations (ITU-R P.1623 –1, 2005). Table 1 lists the statistics of average number of events for different duration during these three years measurement period (2014–2016).

From the Table 1, it is found that as the attenuation threshold increases, the average number of events with a particular duration decreases. Long duration with high attenuation threshold event is rare. This is, in fact, expected and modeled in ITU-R model. It is assumed that statistical distribution of fade duration is independent of location or climatic condition and dependent on rain attenuation threshold which, in turns, dependent on carrier frequency and elevation angle.

Fade duration can be explained by two different types cumulative distribution functions, one is $P(d > D|a > A)$, the probability of occurrence of fades of duration d longer than D (s), given that the attenuation a is greater than A (dB) and another is $F(d > D|a > A)$, the total fraction of fade time due to fades of duration d longer than D, given that the attenuation a is greater than A (dB) as per ITU-R (ITU-R P.1623 –1, 2005). For calculation of fade duration as per ITU-R (ITU-R P.1623 –1, 2005), the important parameters are mean duration(D_0) of the log-normal distribution of the fraction of fading time, standard deviation of the lognormal distribution of the fraction of fading time, and the exponent γ of the power-law distribution of the fraction of fading time. From the above mentioned parameters, total number of fades exceeding the threshold, $N_{tot}(A)$ can be calculated and total time that the threshold is exceeded, $T_{tot}(A)$ can be calculated.

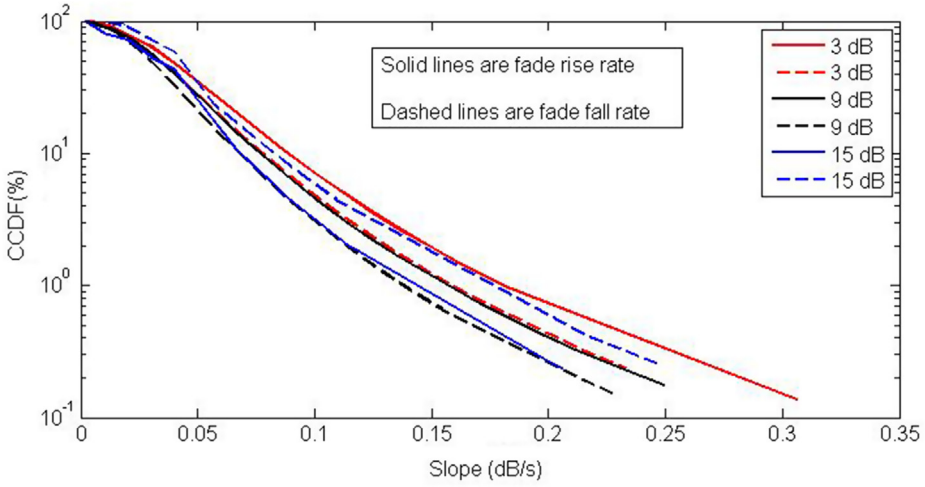

Fig. 5. Complementary Cumulative distribution of fade slope for both fade rise and fade fall for attenuation threshold value of 3 dB, 9 dB, and 15 dB at 20.2 GHz (2014–2016) (Ahmedabad).

Table 1
Average number of occurrences of fade events observed (2014–2016) at different duration for different Attenuation threshold (Ahmedabad).

Duration (sec)	Attn 3 dB	Attn 6 dB	Attn 9 dB	Attn 12 dB	Attn 15 dB
1	195	70	45	32	24
2	161	62	43	31	23
10	122	57	37	28	19
30	99	45	24	16	12
60	84	33	17	15	7
100	69	27	11	11	6
300	35	11	4	2	1
500	27	7	2	2	0
1000	20	2	1	1	0
3000	12	1	1	1	0
5000	7	1	1	1	0

Attempt has been made to study the statistical distribution of fade duration at different attenuation thresholds from 3 dB to 15 dB and is shown in Fig. 6. The figure indicates the average number of events decrease as event duration increases and at lower attenuation threshold, there is a higher number of events present than higher attenuation threshold. Fig. 7 and Fig. 8 show the probability distribution of fade events of the measured data with the distribution obtained from ITU-R (ITU-R P.1623 –1, 2005) and Cheffena-Amaya (Cheffena and Amaya, 2008) model. The Fig. 7 shows that ITU-R model slightly under-estimates the probability of occurrence of mostly short duration fade events.

Cheffena-Amaya also known as CRC model, developed for Ku band is compared with the measured data of Ahmedabad in the Fig. 8. The mean of fade duration due to rain (m_r) and standard deviation of fade duration due to rain (σ_r) are considered as per equation. (3) and (4) of Cheffena-Amaya model.

$$m_r = 689.59 - 173.52\log(f) \tag{3}$$

$$\sigma_r = 0.6210 + 4.3516 * 10^{-3} * f^{1.5} + 3.3637 * A^{-2} \tag{4}$$

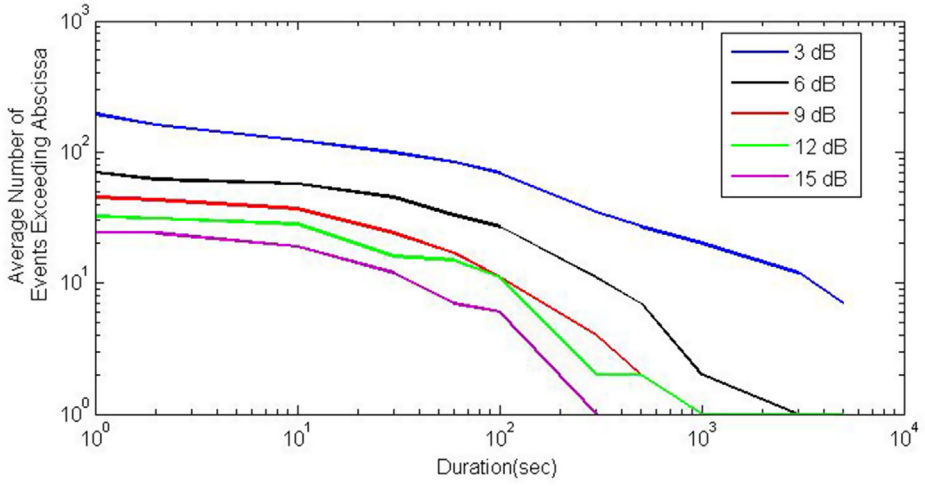

Fig. 6. Average numbers of measured fade events exceeding a given durations (1sec) at 20.2 GHz (2014–2016) (Ahmedabad).

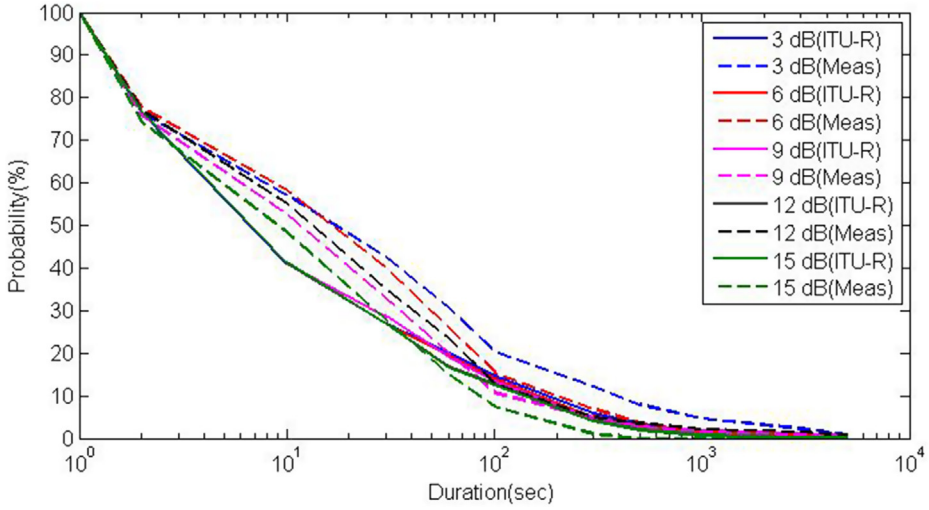

Fig. 7. Comparison of probability of occurrences of fade events between ITU-R model (ITU-R P.1623 –1, 2005) and measured data for given attenuation thresholds at 20.2 GHz (2014–2016) (Ahmedabad).

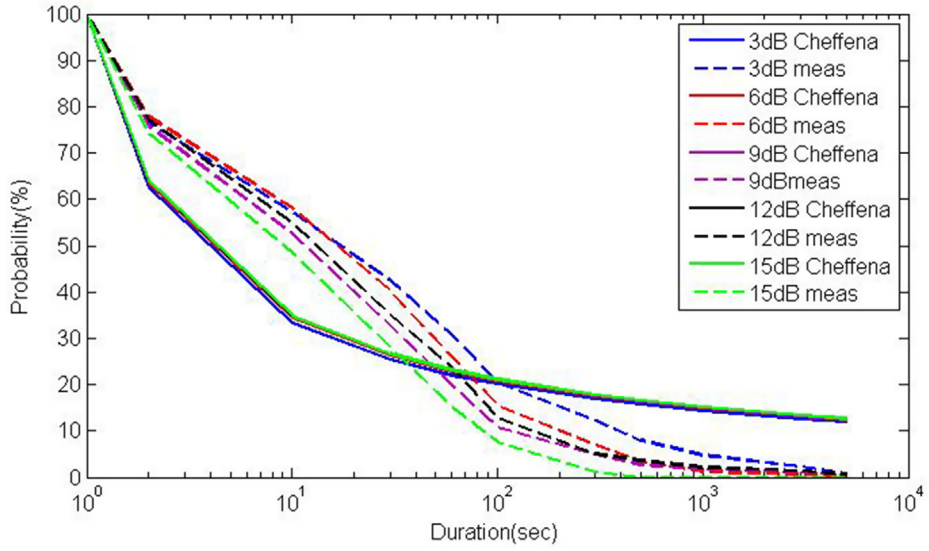

Fig. 8. Comparison of probability of occurrences of fade events between Cheffena model (Cheffena and Amaya, 2008) and measured data for given attenuation thresholds at 20.2 GHz (2014–2016) (Ahmedabad).

Here also the Cheffena-Amaya model under-estimates the probability of occurrence of fade events till 100 s and later overestimates the measured probability of occurrence of fade events for Ahmedabad, India at 20.2 GHz. From Fig. 7 and Fig. 8, discrepancy between measured and modeled probability of occurrence of fade events are observed to be more for Cheffena-Amaya model than ITU-R model.

The total fraction of fade time due to fades of duration d longer than D for different attenuation threshold like 3 dB, 9 dB, 15 dB are plotted in Fig. 9. The distribution shows that fraction of fade times due to fades of duration d longer than D (1 s in our case) is having lower slope at higher attenuation threshold at same value of fade duration.

3.4. Power law exponent of fade duration at Ka band over Ahmedabad

The data collected for the period of three years (2014–2016) over Ahmedabad is plotted for different attenuation threshold to show the attenuation threshold dependence on power law exponent in Fig. 10. It is clearly evident from Fig. 10 that power law exponent (Paraboni and Riva, 1994) of fade duration is dependent on attenuation threshold.

The dependence of power law exponent over attenuation threshold can be quantified from result of three years as

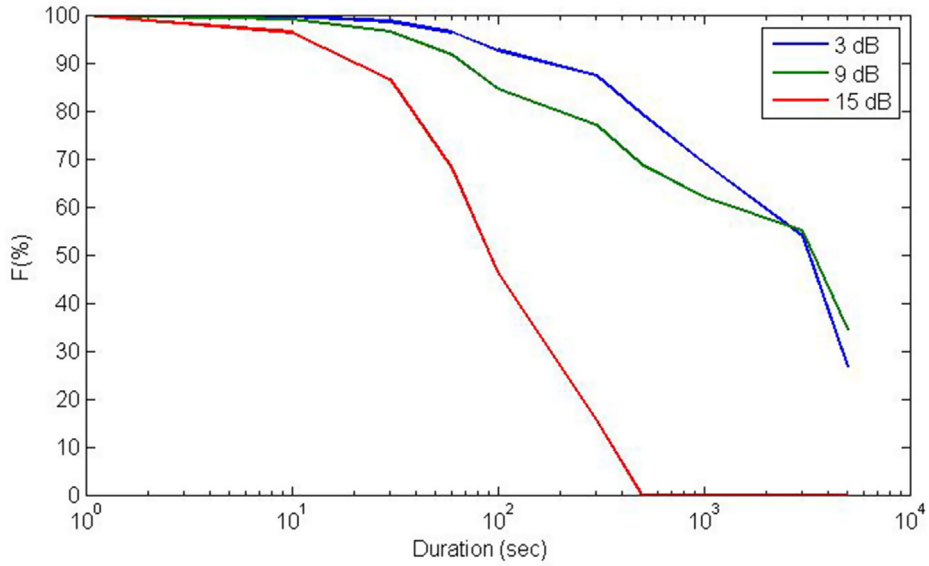

Fig. 9. Cumulative distribution of total fraction of fade time *F(d)* for different attenuation threshold at 20.2 GHz (2014–2016) (Ahmedabad).

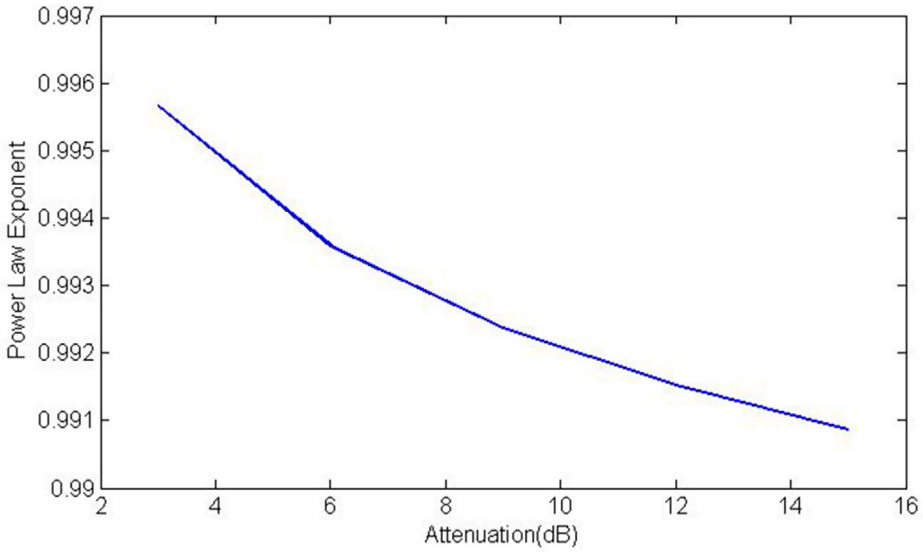

Fig. 10. Variation of power law exponent for various attenuation threshold (dB) at 20.2 GHz (Ahmedabad)(2014–2016).

$$\gamma = 0.143238 * f^{0.65} * (A)^{-0.003} \quad (5)$$

These values of power law exponent are important for ULPC application or FEC application to overcome link outage during heavy rain. Here, the fraction of fading time is plotted for each attenuation threshold for fade duration between 2 to 30 s and later for each attenuation threshold. Power-law exponent of fraction of fading time is then calculated using non– linear curve-fitting tool of MATLAB. The constant value is significantly different from ITU-R (ITU-R P.1623 –1, 2005) as described in the following power law equation (6)

$$\gamma = 0.055 * (f)^{0.65} (A)^{-0.003} \quad (6)$$

3.5. Diurnal analysis of fade duration

As atmospheric temperature has a significant variation in tropical equatorial climate during day time as compared to night times and effect of atmospheric temperature on radio wave propagation is significant, an attempt has been made to evaluate the statistical distribution of event count by dividing the 24 h of a day into four equal parts. The distribution has been plotted in Fig. 11(a) and Fig. 11(b) considering the whole year measurement of 2016 for attenuation threshold of 3 dB and 9 dB. This type of study will help to understand the quality of service (QOS) of SATCOM link during the busiest business hours of the day for the broadcast services.

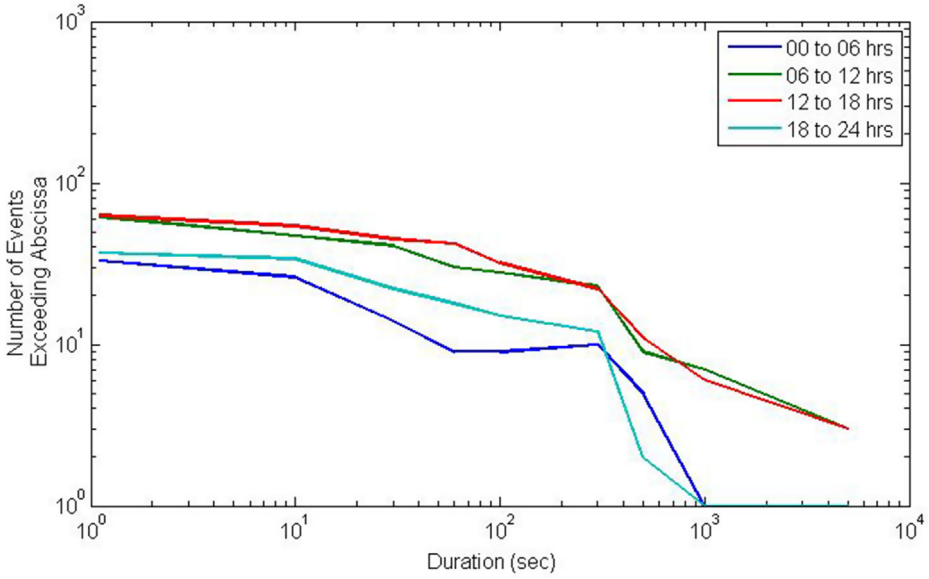

Fig. 11a. Diurnal variation of number of events exceeding abscissa for 3 dB attenuation threshold (2016) (Ahmedabad).

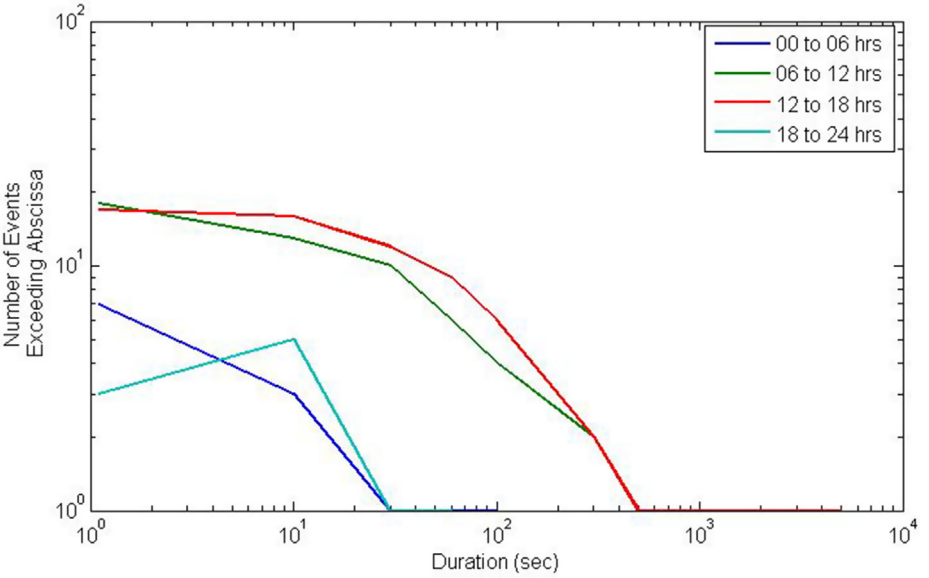

Fig. 11b. Diurnal variation of number of events exceeding abscissa for 9 dB attenuation threshold (2016) (Ahmedabad).

Comparing Fig. 11(a) with Fig. 11(b), it can be concluded that the day time i.e. morning 6 a.m. to 6 p.m., the number of attenuation events are higher for a particular event duration showing even greater value at lower attenuation threshold. Within the day the number of events from 6 a.m. to 12 p.m. and from 12 p.m. to 6 p.m. is sparsely distributed for 9 dB threshold compared to 3 dB thresholds indicating less reliability of the link at higher attenuation threshold. For night time the event count distribution becomes significantly lesser at 9 dB attenuation level as compared to 3 dB attenuation level. This may be due to the fact that during daytime, sun heats the ground and as an effect the air moves up causing more rain during this period. Such information is very important for broadcasting service providers because this is the busiest time for all purpose of communications.

4. New fade duration model

As it is one of the most important designing parameter as per ITU-R (ITU-R P.1623 –1, 2005), an attempt is made to model the standard deviation of the fraction of fading time. The dependence of standard deviation on attenuation threshold has been modeled based on the measurement period of two years (2014–2015) and given by equation (7) as.

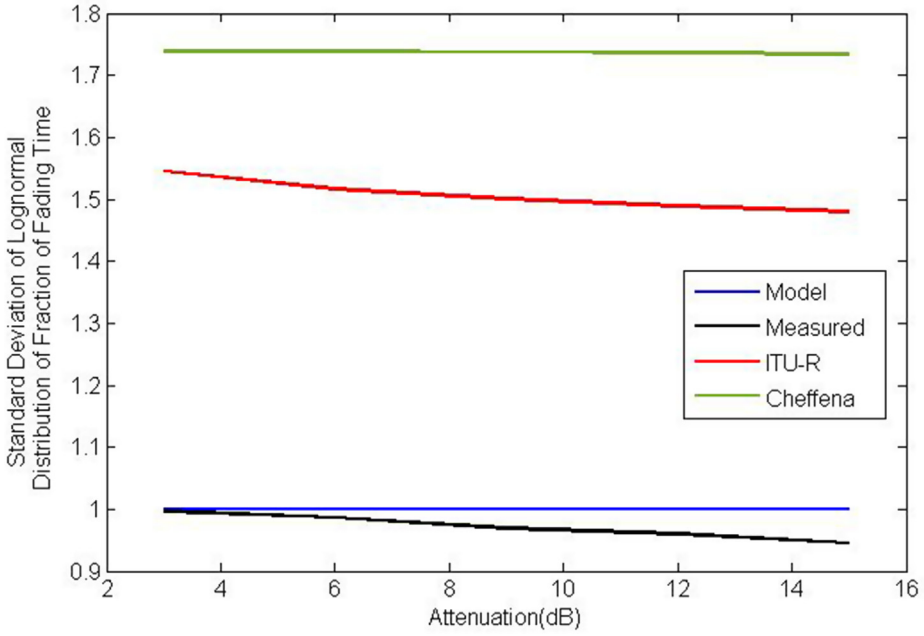

Fig. 12. Comparison of standard deviation of lognormal distribution of the fraction of fading time between new model, ITU-R 1623–1 and Cheffena model for a given attenuation thresholds (Ahmedabad) at 20.2 GHz.

$$\sigma_r = 1.1633 * f^{-0.05} * A^{-0.0004} \quad (7)$$

The coefficients are found to be significantly different from the existing model (Cheffena and Amaya, 2008; ITU-R P.1623 –1, 2005) at Ku band. The same parameter estimated from actual measurements of year 2016 and modeled standard deviation using the proposed model along with ITU-R model and Cheffena-Amaya model are plotted in Fig. 12.

The average of error between measured and modeled standard deviation is maximum of 3% for the event having duration of more than 1 s which is 76% for Cheffena-Amaya model. This may be due to the fact that Cheffena-Amaya model is based on measurements at 11.45 GHz. ITU-R model shows very high error in predicting the standard deviation as shown in the figure.

5. Conclusion

Second order statistics of rain induced attenuation and the deviation of the model parameters from a few popular existing models are presented in this paper for a tropical location, Ahmedabad. Some characteristics of fade slope and fade duration has been studied at Ka band frequency of 20.2 GHz using the received signal for 3 years from GSAT-14 satellite. Asymmetry in fade slope is the significant point observed which indicates the influence of nature of tropical rain over received signal. Analysis of cumulative distribution of fade rise and fade fall further confirms the more frequent presence of Convective rain in tropical regions compared to temperate regions. Relation between the standard deviation of fade duration and attenuation threshold at Ka band for tropical region is also explored. Result shows that long duration event at high attenuation is very rare. The diurnal variations of the fade duration indicate more fading events during daytime than nighttime. Power law exponent of the power law relation of fade duration and attenuation is also investigated and a new model based on the modification of the Cheffena-Amaya (Cheffena and Amaya, 2008) model of standard deviation of log normal distribution of fraction of fading time for Ka band has been attempted. The result indicates that the proposed model performs better than ITU-R model and Cheffena- Amaya model. It is to be, however, noted that the proposed model is presently validated over only a single location and may be used as a local model. All the above information along with further experimental study will be very helpful for SATCOM link designer to devise suitable FMT for the uninterrupted transmission maintaining QOS during heavy rain, especially for tropical regions.

Declaration of Competing Interest

The authors declare that they have no known competing financial interests or personal relationships that could have appeared to influence the work reported in this paper.

Acknowledgment

Authors thankfully acknowledge the scientists of Space Applications Center, ISRO for providing the experimental data. Financial support received under DST- INSPIRE Faculty scheme and ISRO- RESPOND program are also thankfully acknowledged. Authors also express the

gratitude to the anonymous reviewers for immense help with their valuable feedback throughout the work.

References

Allnutt, J.E., Rogers, D.V., 1990. The intelsat slant-path radiowave propagation experiments in tropical regions. Int. J. Satellite Commun. 8 (3), 121–125.

Bråten, L.E., Amaya, C., Rogers, D.V., 2001. Fade and inter-fade duration at Ka band on satellite-earth links: modelling and system implications. 19th International Communications Satellite Systems Conference and Exhibit (ICSSC-19).

Chambers, A.P., Callaghan, S.A., Otung, I.E., 2006. Analysis of rain fade slope for Ka and V-band satellite links in Southern England. IEEE Trans. Antennas Propagat. 54 (5), 1380–1387.

Chakraborty, S., Chakraborty, M., Das, S., 2020. Experimental studies of slant-path rain attenuation over tropical and equatorial regions: a brief review. IEEE Antennas Propag. Mag. https://doi.org/10.1109/MAP.2020. 2976911.

Cheffena, M., Amaya, C., 2008. Prediction model of fade duration statistics for satellite links between 10–50 GHz. IEEE Antennas Wirel. Propag. Lett. 7, 260–263.

Crane, R.K., Robinson, P.C., 1997. ACTS propagation experiment: rain – rate distribution observations and prediction model comparisons. Proc. IEEE. 85 (6), 946.

Dao, H., Islam, M.R.K., Ismail, A.F., 2012. Analysis of rain fade duration over satellite-earth path at Ku-Band in tropics. International Conference on Computer and Communication Engineering (ICCCE 2012), Kuala Lumpur.

Dao, H., Zuhairi, F.A.M., Islam, R.M., 2018. Rain fade duration prediction models for a high elevation angle based on measured data in tropical climate. Adv. Space Res. 62 (7), 1879–1883, 10.1016 /j. asr.2018.06.032.

Das, S., Chakraborty, M., Chakraborty, S., 2020. Experimental studies of Ka Band Rain Fade Slope at a Tropical Location of India. Adv. Space Res. 66 (2020), 1551–1557.

ITU-R Recommendation P.1623–1, 2005. Prediction method of fade dynamics on Earth-space paths.

Jong, S.L., D'Amico, M., Din, J., Lam, H.Y., 2014. Analysis of Fade Dynamic at Ku-Band in Malaysia. Int. J. Antenna Propagat. 2014, 1–7.

Jong, S.L., Riva, C., D'Amico, M., Lam, H.Y., 2019. Fade slope analysis for Ku-band earth-space communication links in Malaysia. IET Microwaves Antennas Propag. 13 (13), 2330–2335.

Kormanyos, Z., Pedersen, L., Sagot, C., & Bito, J., 2000. Rain attenuation and fade duration statistics at 38 GHz derived from long term radio link measurements in Hungary, Norway and Ireland, AP2000 Conference, Davos 13. April 2000.

Lekkla, R., McCormick, K.S., & Rogers, D. V., 1998. 12-GHz fade duration statistics on earth-space paths in South-East Asia. Proceedings of URSI Commission F Open Symposium on Climatic Parameters in Radiowave Propagation Prediction (CLIMPARA '98), Ottawa, Ontario, Canada, 167-170.

Mandeep, J.S., 2013. Fade duration statistics for Ku-band satellite links. Adv. Space Res. 52 (3), 445–450.

Matricciani, E., 1981. Rate of change of signal attenuation from SIRIO at 11.6 GHz. Electron. Lett. 17 (3), 139–141.

Matricciani, E., 1996. Physical-mathematical model of the dynamics of rain attenuation based on rain rate time series and a two-layer vertical structure of precipitation. Radio Sci. 31, 281–295.

Nelson, B., Stutzman, W.L., 1996. Fade slope on 10 to 30GHz earth-space communication links measurements and modeling. IEE Proc.–Microwaves Antennas Propag. 143 (4), 353–357.

Paraboni, A., Riva, C., 1994. A new method for the prediction of fade duration statistics in satellite links above 10 GHz. Int. J. Satellite Commmun. 12, 387–394.

Paraboni, A., Vernucci, A., Zuliani, L., Colzi, E., Martellucci, A., 2007. A new satellite experiment in the Q/V band for the verification of fade countermeasures based on the spatial non-uniformity of attenuation. Proceedings of 2nd European Conference on Antennas and Propagation.

Paulson, K.S., Gibbins, C.J., 2000. Rain models for the prediction of fade durations at millimetre wavelengths. IEE Proc.–Microwave Antennas Propag. 147 (6), 431–436.

Pimienta del Valle, D., Riera, J.M., Garcia-del-Pino, P., Siles, G.A., 2018. Three year fade and inter-fade duration statistics from Q-band Alphasat propagation experiment in Madrid. Int. J. Satell. Commun. Network. 1–17. https://doi.org/10.1002/sat.1271.

Sujimol, M.R., Acharya, R., Singh, G., Gupta, R., 2015. Rain attenuation using Ka and Ku frequency band frequency beacons at Delhi Earth Stations. Indian J. Radio Space Phys. 44, 45–50.

Sweeney, D.G., Bostian, C.W., 1992. The dynamics of rain-induced fades. IEEE Trans. Antennas Propag. 40 (3), 275–278.

Timothy, K.I., Mondal, N.C., Sarkar, S.K., 1998. Dynamical properties of rainfall for performance assessment of earth/space communication links at Ku and Ka bands. Int. J. Satellite Commun.. 16, 53–57.

Timothy, K.I., Ong, J.T., Choo, E.B.L., 2000. Fade and non-fade duration statistics for earth-space satellite link in Ku-band. Electronics Lett. 36 (10), 894–895.

Van de Kamp, M.M.J.L., 2003. Statistical Analysis on rain fade Slope. IEEE Trans. Antennas Propagat. 51 (8), 1750–1759.

Vilhar, A., Kelmendi, A., Hrovat, A., & Kandus, G., 2016. First year analysis of alphasat ka- and q- band beacon measurements in Ljubljana, Slovenia. Ka and Broadband Communications Conference, Ohio, USA, October 2016.

Zemba, M.J., Nessel, J.A., Sia, N., Goussetis, G., 2018. Two years of atmospheric measurements in edinburgh, Scotland, Proceedings of 24th Ka and Broadband Communications Conference. Niagara Falls, Canada.